Development and Evaluation of Real-Time Quantitative PCR Assays for Detection of *Phellinus noxius* Causing Brown Root Rot Disease

Tse-Yen Liu,[1,2] Chao-Han Chen,[2] Yi-Chun Ko,[1] Zong-Chi Wu,[1] Ting-Zhi Liao,[3] Hsin-Han Lee,[4] Isheng Jason Tsai,[4] Tun-Tschu Chang,[2] Meng-Ling Wu,[2] Jyh-Nong Tsai,[5] Ned B. Klopfenstein,[6] Mee-Sook Kim,[7] Jane E. Stewart,[8] Ndeme Atibalentja,[9] Fred E. Brooks,[10] Philip G. Cannon,[11] A. Mohd Farid,[12] Tsutomu Hattori,[13] Hoi-Shan Kwan,[14] Regent Yau Ching Lam,[14,15] Yuko Ota,[16] Norio Sahashi,[13] Robert L. Schlub,[17] Louise S. Shuey,[18] Alvin M. C. Tang,[15,19] and Chia-Lin Chung[1,3,†]

[1] Department of Plant Pathology and Microbiology, National Taiwan University, Taipei 106319, Taiwan
[2] Taiwan Forestry Research Institute, Ministry of Agriculture, Taipei 100051, Taiwan
[3] Master Program for Plant Medicine, National Taiwan University, Taipei 106319, Taiwan
[4] Biodiversity Research Center, Academia Sinica, Taipei 11529, Taiwan
[5] Taiwan Agricultural Research Institute, Ministry of Agriculture, Taichung 413008, Taiwan
[6] United States Department of Agriculture (USDA) Forest Service, Rocky Mountain Research Station, Moscow, ID 83843, U.S.A.
[7] USDA Forest Service, Pacific Northwest Research Station, Corvallis, OR 97331, U.S.A.
[8] Department of Agricultural Biology, Colorado State University, Fort Collins, CO 80523, U.S.A.
[9] American Samoa Community College, Malaeimi 96799, American Samoa
[10] 1961 Westwood Pl., Pomona, CA 91768, U.S.A.
[11] USDA Forest Service, State, Private, and Tribal Forestry, R5 Forest Health Protection, Vallejo, CA 94592, U.S.A.
[12] Forest Health and Conservation Programme, Forest Research Institute Malaysia, Selangor 52109, Kepong, Malaysia
[13] Forestry and Forest Products Research Institute, Tsukuba 305-8687, Japan
[14] School of Life Sciences, The Chinese University of Hong Kong, Hong Kong, China
[15] Muni Arborist Limited, Lam Tsuen, Hong Kong, China
[16] College of Bioresource Sciences, Nihon University, Kanagawa 252-0880, Japan
[17] Cooperative Extension and Outreach, University of Guam, Mangilao 96923, Guam
[18] Department of Agriculture and Fisheries, Queensland Government, Brisbane 4001, Australia
[19] Continuing and Professional Education Division, School of Continuing Education, Hong Kong Baptist University, Hong Kong, China

Abstract

Brown root rot disease (BRRD) is a highly destructive tree disease. Early diagnosis of BRRD has been challenging because the first symptoms and signs are often observed after extensive tissue colonization. Existing molecular detection methods, all based on the internal transcribed spacer (ITS) region, were developed without testing against global *Phellinus noxius* isolates, other wood-decay fungi, or host plant tissues. This study aimed to develop SYBR Green real-time quantitative PCR (qPCR) assays for *P. noxius*. The primer pair Pn_ITS_F/Pn_ITS_R targets the ITS, and the primer pair Pn_NLR_F/Pn_NLR_R targets a *P. noxius*–unique group of homologous genes identified through a comparative genomics analysis. The homologous genes belong to the nucleotide-binding-oligomerization-domain-like receptor (NLR) superfamily. The new primer pairs and a previous primer pair G1F/G1R were optimized for qPCR conditions and tested for specificity using 61 global *P. noxius* isolates, 5 other *Phellinus* species, and 22 non-*Phellinus* wood-decay fungal species. Although all three primer pairs could detect as little as 100 fg (approximately 2.99 copies) of *P. noxius* genomic DNA, G1F/G1R had the highest specificity and Pn_NLR_F/Pn_NLR_R had the highest efficiency. To avoid false positives, the cutoff quantification cycle values were determined as 34 for G1F/G1R, 29 for Pn_ITS_F/Pn_ITS_R, and 32 for Pn_NLR_F/Pn_NLR_R. We further validated these qPCR assays using *Ficus benjamina* seedlings artificially inoculated with *P. noxius*, six tree species naturally infected by *P. noxius*, rhizosphere soil, and bulk soil. The newly developed qPCR assays provide sensitive detection and quantification of *P. noxius*, which is useful for long-term monitoring of BRRD status.

Keywords: comparative genomics analysis, internal transcribed spacer (ITS), molecular diagnosis, nucleotide-binding-oligomerization-domain-like receptor (NLR)

[†]Corresponding author: C.-L. Chung; clchung@ntu.edu.tw

Funding: Support was provided by Taiwan Forestry Research Institute, Ministry of Agriculture, Taiwan; the Office of General Affairs, National Taiwan University; and National Science and Technology Council, Taiwan (grant nos. 109-2313-B-002-045-MY3 and 112-2313-B-002-028-MY3). This work was partially supported by the USDA Forest Service (FS) Research and Development (R&D) Bipartisan Infrastructure Law Ecosystem Restoration Research Project (ERR09), and Forest Service State, Private, and Tribal Forestry, Forest Health Protection—Special Technology Development Program.

e-Xtra: Supplementary material is available online.

The author(s) declare no conflict of interest.

Accepted for publication 25 June 2024.

© 2024 The American Phytopathological Society

Brown root rot disease (BRRD), caused by *Phellinus noxius* (Corner) G. Cunningham, is a highly destructive tree disease prevalent in tropical and subtropical regions. Although *P. noxius* was once proposed to be renamed *Pyrrhoderma noxium*, the suggestion was based on specimens from fallen unidentified angiosperm trunks in Hainan, China (Zhou et al. 2018), without referring to the type material. A recent phylogenetic analysis revealed that isolates identified as *P. noxius* from Taiwan, Malaysia, Japan, China, Singapore, Thailand, India, and Costa Rica belong to the same clade (global *P. noxius*) but are distinct from the clade of *Py. noxium* isolates from China (China *Py. noxium*) (Leung et al. 2020). Hosts of *P. noxius* include more than 200 tree species from 59 different families representing both broad-leaved and coniferous species, as well as certain herbaceous species (Ann et al. 2002; Chen et al. 2023; Hsiao et al. 2019). Spread of *P. noxius* to neighboring trees primarily occurs through infected roots, and long-distance spread occurs via airborne

basidiospores (Ann et al. 2002; Chung et al. 2015, 2017). Wood decay follows after *P. noxius* invades the cortex and lignified xylem (Chang 1992). The degradation of root tissues results in a substantial reduction in a tree's physical support and its ability to uptake water and nutrients (Ann et al. 2002; Cherubini et al. 2002). For this reason, BRRD-afflicted trees with decayed roots are prone to structural failure and/or toppling over. The economic losses and potential hazards to public safety caused by BRRD are of particular concern in densely populated urban areas.

Conventional diagnosis of BRRD is done by observing the symptoms or signs in the advanced stages of disease. BRRD-afflicted trees typically show aboveground symptoms, such as sparse leaves, abnormal yellowing of leaves, and defoliation, and the infected roots show white rot symptoms. Typical signs of BRRD include brown to black mycelial mats covering basal trunks and roots, with a network of dark brown mycelial cords on decayed woody tissues. Occasionally, flat (resupinate) or bracket fruiting bodies with gray to brown hymenial layer containing irregular polygonal pores can be observed (Ann et al. 2002; Hsiao et al. 2019). The selective medium MA+4 (malt extract agar plus benomyl, dicloran, chloramphenicol, and gallic acid) was developed for *P. noxius* isolation and preliminary identification (Chang 1996). Gallic acid in the selective medium is oxidized by *P. noxius* to produce a characteristic dark reddish-brown diffusion zone around its colony (Chang 1996; Davidson et al. 1938). A more detailed morphological identification of *P. noxius* requires subculturing the colony onto potato dextrose agar (PDA) (Chang 1992). However, it is typically difficult to diagnose BRRD in a timely manner because the aboveground symptoms are usually observed at the later stages of infection and the process of isolation and culturing is time-consuming. In addition, both visual inspection and morphological identification rely on expertise and experience.

For rapid and accurate diagnosis of BRRD, several molecular detection methods have been developed based on sequences of the internal transcribed spacer (ITS) region of ribosomal DNA. Tsai et al. (2007) designed a specific primer pair PN-1F/PN-2R for PCR detection of *P. noxius* by comparing the ITS regions of 18 *P. noxius* isolates, 7 isolates of other *Phellinus* species, and 7 isolates of other wood-decay fungi. PN-1F/PN-2R amplifies 414- or 422-bp amplicons for different *P. noxius* isolates. Wu et al. (2009) designed another PCR primer pair for *P. noxius*, G1F/G1R, by sequencing the ITS of 9 different *Phellinus* species, and 16 *P. noxius* isolates were used to confirm the specificity of G1F/G1R. G1F/G1R amplifies a single 653-bp band and is currently widely used for *P. noxius* detection (Wu et al. 2011). To enhance the sensitivity of *P. noxius* detection, Wu et al. (2011) subsequently developed a nested PCR assay using the primer pair G1F/G1R and an inner primer G1R2. In two recent studies, G1F/G1R and G1F/G1R2 were used for real-time quantitative PCR (qPCR) assays without comprehensive evaluations for efficiency, specificity, and sensitivity (Liu et al. 2022; Wang et al. 2016). Furthermore, Huang et al. (2014) developed a loop-mediated isothermal amplification assay that can differentiate *P. noxius* from the 8 other *Phellinus* species, and Tzean et al. (2016) developed a high-throughput oligonucleotide microarray system that allowed 17 different species of *Phellinus* to be distinguished simultaneously. Because all of these existing detection methods were developed and tested with only *P. noxius* isolates from Taiwan, additional assessments are needed to determine whether these methods can distinguish diverse global isolates of *P. noxius* from diverse host plants and wood-decay fungi of other genera.

The development of high-throughput sequencing technology has produced extensive sequence data of *P. noxius* isolates ranging from partial DNA regions to whole genomes. Analysis of the ITS sequences of 58 isolates belonging to 39 *Phellinus* species showed that all *P. noxius* isolates were monophyletic (Tsai et al. 2017). Among 91 *P. noxius* isolates from Taiwan, the ITS lengths were classified into the long (L), medium (M), and short (S) types, and the three types were further divided into L1, M1 to M33, and S1 to S2 subtypes based on 20 distinct variations of single-nucleotide polymorphisms (SNPs) and insertion and deletions (indels) (Tsai et al. 2017). Multilocus phylogenetic analysis of the nuclear large subunit, ITS, partial RNA polymerase II, and partial translation elongation factor 1-alpha of 95 *P. noxius* isolates from 12 different countries/regions revealed the presence of three distinct lineages that might be associated with specific climatic niches (Stewart et al. 2020). Comparative and population genomics analyses of 60 *P. noxius* isolates from Taiwan and Japan (Ryukyu and Ogasawara islands) showed that *P. noxius* are hypervariable multinucleate species with their genomes containing abundant poly-allelic SNPs (Chung et al. 2017). Recently, Kozhar et al. (2022) found distinct population structure and patterns of genetic variation in *P. noxius* isolates from diverse global regions. The high genetic diversity in the *P. noxius* genome and its ITS region demonstrates the need to reexamine previously developed detection methods.

In this study, qPCR assays for *P. noxius* detection and quantification were developed. For primer design, we targeted ITS and unique genetic regions of *P. noxius* identified through a comparative genomics analysis. Two newly developed primer pairs and a previously developed primer pair, G1F/G1R, were optimized for qPCR conditions and tested for specificity using global *P. noxius* isolates and common wood-decay fungi. The qPCR assays were validated using artificially inoculated *Ficus benjamina* seedlings and naturally infected field samples. The new qPCR assays are expected to provide more accurate detection of *P. noxius* with utility for long-term monitoring of BRRD status.

Materials and Methods

Fungal isolates and cultivation

In total, 89 isolates of 12 wood-decay fungal genera were used in this study. These included 61 *P. noxius* isolates from different geographic regions (Chou et al. 2019; Chung et al. 2017; Liao et al. 2023), 5 other *Phellinus* species (i.e., *P. apiahynus*, *P. hoehnelii*, *P. igniarius*, *P. laevigatus*, and *P. quercinus*), and 23 isolates of 11 other common wood-decay fungal genera (i.e., *Antrodia*, *Coriolopsis*, *Earliella*, *Ganoderma*, *Heterobasidion*, *Polyporus*, *Pycnoporus*, *Rigidoporus*, *Schizophyllum*, *Trametes*, and *Xylobolus*). Details and sources of these isolates are available in Supplementary Table S1. Each isolate was revived by culturing on PDA (HiMedia, India) for 7 days at 25°C in the dark and then subcultured on 2% malt extract agar (HiMedia, India) for 10 days at 25°C in the dark. The identity of each isolate was confirmed by morphological characteristics and ITS sequences. The ITS regions were amplified with ITS5/ITS4 primers (White et al. 1990), Sanger sequenced by Genomics (New Taipei City, Taiwan), and searched against the NCBI GenBank nr/nt database using BLAST, with searches restricted to type materials (Altschul et al. 1997; Thompson et al. 1994).

DNA extraction

Fungal mycelium was collected from 7- to 10-day-old colonies, frozen in liquid nitrogen, and ground to a fine powder with a sterile mortar and pestle. The genomic DNA was extracted using the Yeast Genomic DNA Kit (Geneaid Biotech, Taiwan) following the manufacturer's instructions. For genomic DNA extraction from bulk soil and rhizosphere soil samples, the DNeasy PowerSoil Kit (Qiagen, Hilden, Germany) was used following the manufacturer's instructions.

Plant genomic DNA was extracted from wood tissues. To eliminate the influence of secondary metabolites and protein inhibitors on DNA quality and yield, the extraction was conducted following modified protocols of Fatima et al. (2018) and Inglis et al. (2018). The frozen tissues were ground into a fine powder in liquid nitrogen using a sterile mortar and pestle. Approximately 0.1 mg of the ground tissues was mixed with 1 ml of sorbitol wash buffer (100 mM Tris-HCl [pH 8.0], 300 mM sorbitol, 5 mM EDTA [pH 8.0], and 1% [wt/vol] polyvinylpyrrolidone [average molecular weight 40,000; PVP-40]) and centrifuged at 2,500 × *g* for 15 min at room temperature. After removing the supernatant, 1 ml of prewarmed 3.5× CTAB lysis buffer (100 mM Tris-HCl [pH 8.0], 1.4 mM NaCl, 3.5% CTAB [cetyl trimethylammonium bromide], 20 mM EDTA, and 2.5% [wt/vol] PVP-40) were added. The sample was incubated at

65°C for 50 to 60 min with inversion every 10 min. After adding 1 ml of chloroform:isoamyl alcohol (24:1 vol/vol; CIA) and shaking vigorously, the sample was centrifuged at 2,500 to 5,000 × *g* for 10 min at room temperature, and the upper aqueous phase was transferred to a new tube. The CIA extraction step was repeated if the upper aqueous phase was light tan. The sample was gently mixed with 0.66 volumes of cold isopropanol and kept at 4°C for 1 h. After centrifuging at 13,000 × *g* for 15 min at 4°C, the supernatant was removed. The DNA pellet was washed twice with 500 µl of 70% ethanol and once with 100% ethanol, dried at room temperature for 1 h, then gently suspended in 30 µl of double-distilled water (ddH_2O). DNA samples were stored at −20°C before further assays.

Target region selection and primer design

To design ITS-based qPCR primers, the ITS sequences of 41 global *P. noxius* isolates and 29 other *Phellinus* species were downloaded from the NCBI database (Supplementary Table S2). These included two representative ITS sequences from the annotated genome of *P. noxius* FFPRI411160 (CM008257.1: 301,777 to 302,423 and 311,762 to 312,408 bp) (Chung et al. 2017) and six ITS sequences belonging to three major ITS types of the *P. noxius* population in Taiwan (Type L: JQ003239.1; Type M: JQ003233.1, JN836346.1, and JQ029276.1; Type S: JQ003236.1 and JQ003237.1) (Tsai et al. 2017) (Fig. 1A).

To identify the genetic region(s) unique to *P. noxius*, phylogenetic orthology was inferred using OrthoFinder version 1.0.6 (Emms and Kelly 2015). The FASTA files for peptide sequences of 61 representative fungal genomes were obtained from the JGI MycoCosm or NCBI database (Supplementary Table S3). Pairwise comparisons were performed to cluster the orthogroups across the fungal genomes, which led to the identification of a unique group of homologous genes in *P. noxius*. A 3,776-bp fragment of the homologous genes (full length ~3,804 bp) was amplified from *P. noxius* isolates B98 and 2248 using Pn_Fwd (5′-CAGACCAACACAACAATC-3′) and Pn_Rev (5′-TGTCGTCTCTTAATTCCC-3′) (Fig. 1B). The amplicons were cloned into the pGEM-T Easy Vector (Promega Corporation, U.S.A.) and then transformed into *Escherichia coli* JM109 competent cells (Promega Corporation, U.S.A.) following the manufacturer's instructions. Each clone was sequenced using M13F and M13R primers and by primer walking by Tri-I Biotech (New Taipei City, Taiwan).

Multiple sequence alignment was performed using MAFFT v. 7 (Katoh et al. 2002, 2019). The aligned sequences were visually inspected to identify intraspecies consensus and interspecies variable sequences for primer design. The melting temperature, G/C content, and other thermodynamic parameters were calculated using Primer-Premier 5 (Premier Biosoft Interpairs, Palo Alto, CA) and Primer3Plus v. 2.4.0 software (Untergasser et al. 2007). The specificity of selected primer pairs was evaluated using primer-BLAST (Ye et al. 2012) against the NCBI nr database with all organisms. The *P. noxius*-specific primers without mismatches to unintended targets at the 3′ end were selected. Table 1 shows the sequences of two newly designed primer pairs and the G1F/G1R primer pair designed by Wu et al. (2009). G1F/G1R was included in our tests owing to its widespread use in *P. noxius* detection. The primer positions are shown in Figure 1.

Efficiency, specificity, and sensitivity of the real-time qPCR assay

All qPCR assays were performed with the CFX Connect Real-Time PCR Detection System (Bio-Rad, CA, U.S.A.). The two-step thermal cycling parameters were 95°C for 2 min followed by 40 cycles of 95°C for 5 s and an optimal annealing/extension temperature of 65 or 68°C for 20 s. The reaction of each qPCR assay was in 10 µl containing 1 µl of genomic DNA (DNA concentration depends on the purpose of the test; please see below), 5 µl of 2× qPCRBIO SyGreen Blue Mix (PCR Biosystems, U.K.), 1 µl of 5 µM forward and reverse primers each, and 2 µl of ddH_2O.

To determine the amplification efficiencies of each primer pair at different annealing/extension temperatures, a gradient qPCR was performed in three technical replicates with a 10-fold serial dilution of the *P. noxius* 2248 genomic DNA (1 ng/µl to 0.1 fg/µl). The efficiency was calculated using the following equation: $E = -1 + 10^{(-1/\text{slope})}$ (Broeders et al. 2014). The specificity assays were performed in three technical replicates using 1 ng/µl of the genomic DNA of 89 fungal isolates. These included 61 *P. noxius* isolates from different countries/regions, 5 other *Phellinus* species, and 22 wood-decay fungal species belonging to 11 other genera (Supplementary Table S1). To examine nonspecific signals, an additional three independent experiments were conducted for non–*P. noxius* organisms.

The sensitivity assays were performed using a 10-fold serial dilution of the *P. noxius* 2248 genomic DNA (1 ng/µl to 0.1 fg/µl). The DNA concentration was determined using the NanoDrop Lite Spectrophotometer (Thermo Fisher Scientific, MA, U.S.A.). The sensitivity was represented by the limit of detection (LOD), defined as the minimum concentration detectable. The qPCR assays were performed three times with five replicates for each DNA concentration, and the LOD was determined as the lowest concentration that yielded positive results in all replicates. The cutoff for the quantification cycle (Cq) value was determined as "the Cq value corresponding to the LOD" (Caraguel et al. 2011). Any Cq values above the cutoff were unreliable and considered negative signals.

qPCR analysis of *P. noxius* in infected plant tissues

The qPCR assays were tested using artificially inoculated and naturally infected samples. The branches of *Ficus benjamina* seedlings were used for inoculation with *P. noxius* 2248. To prepare the inoculum, *P. noxius* 2248 was cultured on PDA for 5 days, transferred to autoclaved wheat-oat grains (50 g of wheat grains, 50 g of oat grains, 50 ml of ddH_2O, and 100 µg/ml of chloramphenicol), and then incubated in the dark at 30°C for 2 weeks (Ann et al. 2002; Chou et al. 2019). The branches were gently wounded by scraping the epidermis, and then ca. 8 g of the inoculum was wrapped around the wounded area using Parafilm. The inoculation was conducted on three plants, each treated with the *P. noxius* inoculum on five branches. The other three plants, each treated with autoclaved wheat-oat grains on five branches, were used as the control. The experiment was performed at 30°C/30°C day/night temperature at the Phytotron of National Taiwan University in June 2023. At 3, 5, 7, 10, and 14 days postinoculation (dpi), three replicates of inoculated and control branches were collected from each of the three plants and stored at −20°C before DNA extraction. DNA extraction and qPCR assays were conducted as described above. The standard curve for inoculated tissues was generated using 1 µl of 50 ng/µl per *F. benjamina* genomic DNA mixed with 1 µl of a 10-fold serial dilution of the *P. noxius* 2248 genomic DNA (1 ng/µl to 0.1 fg/µl) per reaction (Chen et al. 2020). The efficiency and sensitivity were determined as described above. Differences among the amounts of *P. noxius* in *F. benjamina* tissues at different dpi were analyzed by analysis of variance and Tukey's honestly significant difference test at $P < 0.05$, using the 'agricolae' package in R version 4.1.2 (de Mendiburu 2014).

Field samples were collected from 10 diseased trees of *Bischofia javanica*, *Camphora officinarum*, *Ficus microcarpa*, *Koelreuteria elegans*, *Salix babylonica*, and *Zelkova serrata* at National Taiwan University (NTU), Taipei Botanical Garden, and Feitsui Reservoir. Root samples were collected from two or four different cardinal directions of each tree. For two neighboring *S. babylonica* trees at NTU, bulk soil samples were collected from around the roots and between the two trees. For a *C. officinarum* tree at NTU, bulk soil and rhizosphere soil samples were collected. Branch samples of each tree were collected to serve as negative controls. DNA extraction and qPCR assays were conducted as described above. The reaction of each qPCR assay was in 10 µl containing 1 µl of genomic DNA (10 ng/µl), 5 µl of 2× qPCRBIO SyGreen Blue Mix (PCR Biosystems, U.K.), 1 µl of 5 µM forward and reverse primers each, and 2 µl of ddH_2O.

Tissue isolation was conducted to confirm the infection by *P. noxius*. Plant tissues were surface-disinfested with 75% ethanol for 30 s, rinsed with sterile deionized water three times, then cultured on

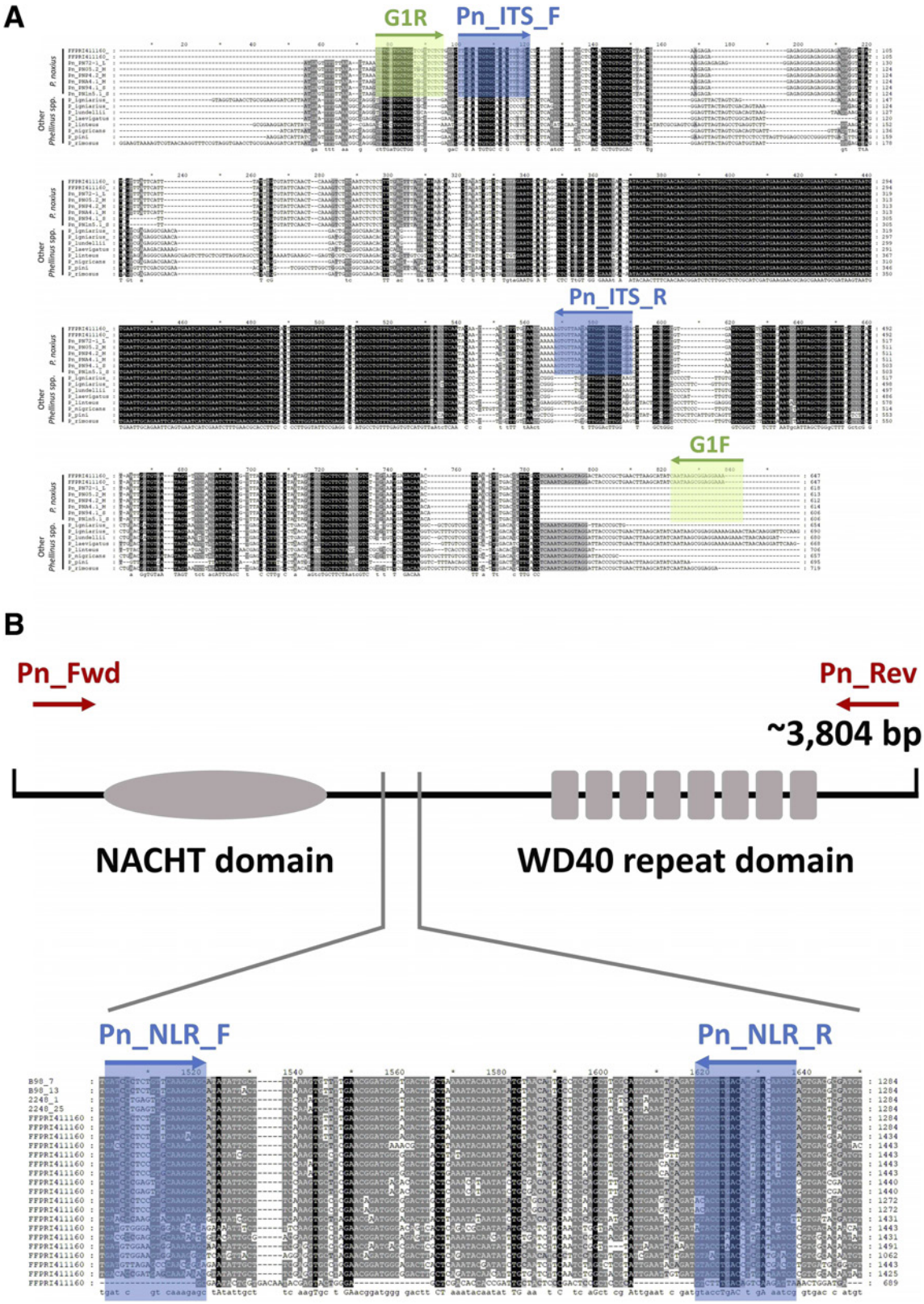

Fig. 1. Genetic positions of three primer pairs used in this study. **A,** Alignment of partial internal transcribed spacer (ITS) sequences of eight isolates of *Phellinus noxius* and eight other *Phellinus* species (*P. pini*, *P. laevigatus*, *P. igniarius*, *P. lundellii*, *P. rimosus*, *P. nigricans*, *P. cinereus*, and *P. linteus*). **B,** The schematic diagram and partial sequences of a *P. noxius*–unique group of homologous genes (full length ca. 3,804 bp), which belong to the nucleotide-binding-oligomerization-domain-like receptor (NLR) superfamily. Primer pairs Pn_ITS_F/Pn_ITS_R and Pn_NLR_F/Pn_NLR_R (shaded boxes under respective labels with arrows) were designed in this study, and G1F/G1R (shaded boxes under respective labels with arrows) was designed by Wu et al. (2009). The primer pair Pn_Fwd/Pn_Rev (labeled with arrows) was used to clone a 3,776-bp fragment of the NLR sequences from *P. noxius* 2248 and B98.

a modified *P. noxius*–selective medium, MA+4 (20 g of malt extract, 20 g of agar, 10 mg of benomyl, 10 mg of dicloran, 100 mg of chloramphenicol, and 500 mg of gallic acid per 1 liter), for 3 to 5 days (Chang 1995; Wu et al. 2020).

Results

Identification of *P. noxius*–specific regions for primer design

The ITS sequences of *P. noxius* and other *Phellinus* species were aligned to identify *P. noxius*–specific regions for primer design. For the primer pair Pn_ITS_F and Pn_ITS_R, SNPs and indels were found between *P. noxius* and other *Phellinus* species. A 415-bp product was amplified from *P. noxius* (Table 1; Fig. 1A). The comparative genomics analysis identified only one unique group of 84 homologous genes in the genome of *P. noxius* FFPRI411160. These genes, belonging to the nucleotide-binding-oligomerization-domain-like receptor (NLR) superfamily, were randomly distributed in the genome. The NLR superfamily is characterized by the NACHT (also known as the P-loop NTPase) and multiple WD40 repeat domains (Dyrka et al. 2014; Proell et al. 2008). After excluding the highly conserved NACHT and WD40 domains, the remaining NLR sequences were used for primer design. The template NLR region did not match any sequences of other fungal species through analysis of NCBI BLASTN. The primer pair Pn_NLR_F and Pn_NLR_R that produced a 131-bp amplicon was designed for further qPCR assays (Table 1; Fig. 1B).

Efficiency, specificity, and sensitivity of the qPCR assays

Two newly designed primer pairs, Pn_ITS_F/Pn_ITS_R and Pn_NLR_F/Pn_NLR_R, and the previously designed primer pair, G1F/G1R, were tested for optimal qPCR conditions, efficiency, specificity, and sensitivity (Table 1; Supplementary Table S4). The optimal annealing/extension temperatures for G1F/G1R, Pn_ITS_F/Pn_ITS_R, and Pn_NLR_F/Pn_NLR_R were determined to be 65, 68, and 65°C, respectively. The coefficient of determination (R^2) values for qPCR standard curves for 10-fold serial dilutions of *P. noxius* DNA were >0.99 for all three primer pairs (Assay 1 in Fig. 2). The efficiency of Pn_NLR_F/Pn_NLR_R (95.8%) was better than that of G1F/G1R (83%) and Pn_ITS_F/Pn_ITS_R (83.7%). The LOD values for all three primer pairs were determined to be 100 fg (approximately 2.99 copies) of *P. noxius* genomic DNA. The cutoff Cq values were 34 for G1F/G1R, 29 for Pn_ITS_F/Pn_ITS_R, and 32 for Pn_NLR_F/Pn_NLR_R (Supplementary Table S4).

Among the 89 fungal isolates tested, all 61 *P. noxius* isolates from different geographical regions could be detected (Cq = 16.2 to 28.0), whereas the other 28 fungal isolates belonging to 27 fungal species were not detected (Table 2). Notably, a nonspecific signal of G1F/G1R against *Coriolopsis aspera* was detected at a Cq value of approximately 25. The amplicon has a melting temperature (Tm) of 85°C and could be distinguished from the amplicon of *P. noxius* (Tm = 82.0 to 82.5°C). Nonspecific signals with Cq values >33.7 were detected for G1F/G1R against *Ganoderma fornicatum* (with a frequency of 100%), Pn_ITS_F/Pn_ITS_R against *Earliella scabrosa*, *Pycnoporus sanguineus*, *Rigidoporus ulmarius*, and *Schizophyllum commune* (with a frequency of 67 to 100%), and Pn_NLR_F/Pn_NLR_R against *Phellinus apiahynus*, *Schizophyllum commune*, and *Rigidoporus ulmarius* (with a frequency of 25 to 33%). Although the Tm values of most nonspecific signals are indistinguishable from those of *P. noxius*, their Cq values exceeded the cutoff values and could therefore be correctly determined as negative signals.

Validation of the qPCR assays with artificially inoculated *F. benjamina* tissues

The R^2 values for qPCR standard curves for 10-fold serial dilutions of *P. noxius* DNA mixed with 50 ng of *F. benjamina* DNA were >0.99 for all three primers (assay 2 in Fig. 2). The LOD values of all three primer pairs were 100 fg. The amplification curves, qPCR efficiencies, and cutoff Cq values were consistent with those of the assays using only *P. noxius* DNA (Fig. 2; Supplementary Table S4). The consistency suggests no discernible influence of *F. benjamina* DNA on the qPCR performance. However, nonspecific signals were occasionally observed for the negative control (*F. benjamina* DNA) with Cq values >34, 29, and 32 for G1F/G1R, Pn_ITS_F/Pn_ITS_R, and Pn_NLR_F/Pn_NLR_R, respectively. These false-positive signals could be excluded by applying the cutoff Cq values determined for each primer pair.

For the inoculated *F. benjamina* branches, BRRD symptoms and the amount of *P. noxius* were monitored over 2 weeks. The leaves and branches started to wilt at 3 dpi. Wilting and chlorosis symptoms were evident at 5 dpi and became more severe at 7 to 14 dpi (Fig. 3A). For all *P. noxius*–inoculated branches, *P. noxius* was successfully isolated at all time points. For the three primer pairs, the changes in the estimated biomass of *P. noxius* over time were consistent. From 1 ng of total DNA extracted from the infected tissues, *P. noxius* was found as a trace amount at 3 dpi (253 to 957 fg). The amount of *P. noxius* DNA increased significantly at 5 dpi (113 to 367 pg) and reached the highest amount at 7 dpi (199 to 511 pg) (Fig. 3B). From 7 to 14 dpi, although the wilting symptom became more severe over time, the amounts of *P. noxius* showed a decreasing trend for all three primer pairs. With G1F/G1R and Pn_ITS_F/Pn_ITS_R, the amount of *P. noxius* was significantly lower at 14 dpi than 7 dpi. No significant differences were detected at 7, 10, and 14 dpi when using Pn_NLR_F/Pn_NLR_R.

Application of the qPCR assays for field samples

The results of qPCR assays for the roots, bulk soil, and rhizosphere soil samples of field trees (A to P) are in Table 3. The Cq values below the cutoff (34 for G1F/G1R, 29 for Pn_ITS_F/Pn_ITS_R, and 32 for Pn_NLR_F/Pn_NLR_R) were determined as positive detection of *P. noxius*. The results of the three primer pairs were generally consistent. For samples of trees A to C and E to J showing BRRD symptoms or signs, *P. noxius* was detected in 97% of the decayed root samples by all three qPCR assays and tissue isolation (among 33 decayed root samples, only B1 tested negative). For the decayed root samples from tree D (tissue isolation not tested), whereas *P. noxius* was detected in samples D1 to D3 by all three primer pairs, sample D4 was determined as negative using G1F/G1R (Cq = 34.7, close to the cutoff value 34) and Pn_ITS_F/Pn_ITS_R (Cq = 31.4) but as positive using Pn_NLR_F/Pn_NLR_R (Cq = 31.3, close to the cutoff value 32). In contrast, *P. noxius* was not

Table 1. The primers used for quantitative real-time PCR

Primer	Target	Sequences (5′–3′)	Product size (bp)	Annealing/ extension temperature	Efficiency (%)	Limit of detection	Reference
G1F	Internal transcribed spacer (ITS)	GCCCTTTCCTCCGCTTATTG	653	65	83	100 fg	Wu et al. 2009
G1R		CTTGATGCTGGTGGGTCTCT					
Pn_ITS_F		TTGCATGTGCTCAGTTTGCG	415	68	83.7	100 fg	This study
Pn_ITS_R		TCCCCAAGTCCAATATTAACACT					
Pn_NLR_F	Nucleotide-binding-oligomerization-domain like receptor (NLR)	GATCCCTCTGTTCAAAGAGC	131	65	95.8	100 fg	This study
Pn_NLR_R		CGATTGTCGATGTCAGGTAC					

detected in any root samples from the healthy trees K to P using all three qPCR assays. Nonspecific signals were not detected for any of the negative controls (branch samples of *B. javanica*, *C. officinarum*, *F. microcarpa*, *K. elegans*, *S. babylonica*, and *Z. serrata*). Notably, the amounts of *P. noxius* DNA varied largely in different root samples from the same diseased tree, regardless of whether the diseased tree displayed aboveground symptoms. For example, only one of four root samples of tree A (A1) and only three of four root samples of tree B (B2 to B4) tested positive.

DNA of *P. noxius* was detected in all four rhizosphere soil samples (C1_RS to C4_RS) and one of 12 bulk soil samples (C1_BS). The amounts of *P. noxius* DNA in the rhizosphere soils (Cq = 18.8 to 27.7) were ca. 10 times lower than the amounts in the corresponding roots (Cq = 14.5 to 23.3). Only a trace amount of *P. noxius* DNA was detected in the bulk soil sample C1_BS (Cq = 28.2 to 30.7).

Discussion

Real-time quantitative PCR is a specific, sensitive, and time-efficient technique for diagnosis and quantification of plant pathogens (Hariharan and Prasannath 2020; McCartney et al. 2003). To detect *P. noxius* in root tissues and soil, Wang et al. (2016) and Liu et al. (2022) conducted qPCR using G1F/G1R and G1F/G1R2, which were derived from two ITS-based primer pairs designed for conventional PCR. However, these primer pairs were used without comprehensive evaluations for optimal conditions, efficiency, specificity, and sensitivity. In this study, comparative genomics analysis and in silico analysis were conducted to identify *P. noxius*–specific regions. Two newly designed primer pairs, Pn_ITS_F/Pn_ITS_R and Pn_NLR_F/Pn_NLR_R, and the widely used G1F/G1R were tested for optimal qPCR conditions and LOD values. The specificity was evaluated using a total of 61 *P. noxius* isolates, 5 other *Phellinus* species, and an additional 22 non-*Phellinus* wood-decay fungal species. Among the three primer pairs tested, G1F/G1R showed the highest specificity, and Pn_NLR_F/Pn_NLR_R showed the highest overall efficiency. It should be noted that the qPCR assays developed in this study aimed at detecting global *P. noxius*. Because China *Py. noxium* sample was not included in our tests, the specificity of G1F/G1R, Pn_ITS_F/Pn_ITS_R, and Pn_NLR_F/Pn_NLR_R for China *Py. noxium* remained undetermined.

The ITS region, known for its interspecific variation (Schoch et al. 2012), has been commonly used for identification in fungal taxonomy at the genus/species level. Although variations in the length and sequences of ITS were identified among different *P. noxius* isolates (Chung et al. 2017; Tsai et al. 2017), it has proved to be an effective target for designing *P. noxius*–specific primers. Chitin synthase, actin, and calmodulin are also widely used for primer design in plant pathogen detection (Chung et al. 2022; Prencipe et al. 2023); however, publicly available sequence information is quite limited for

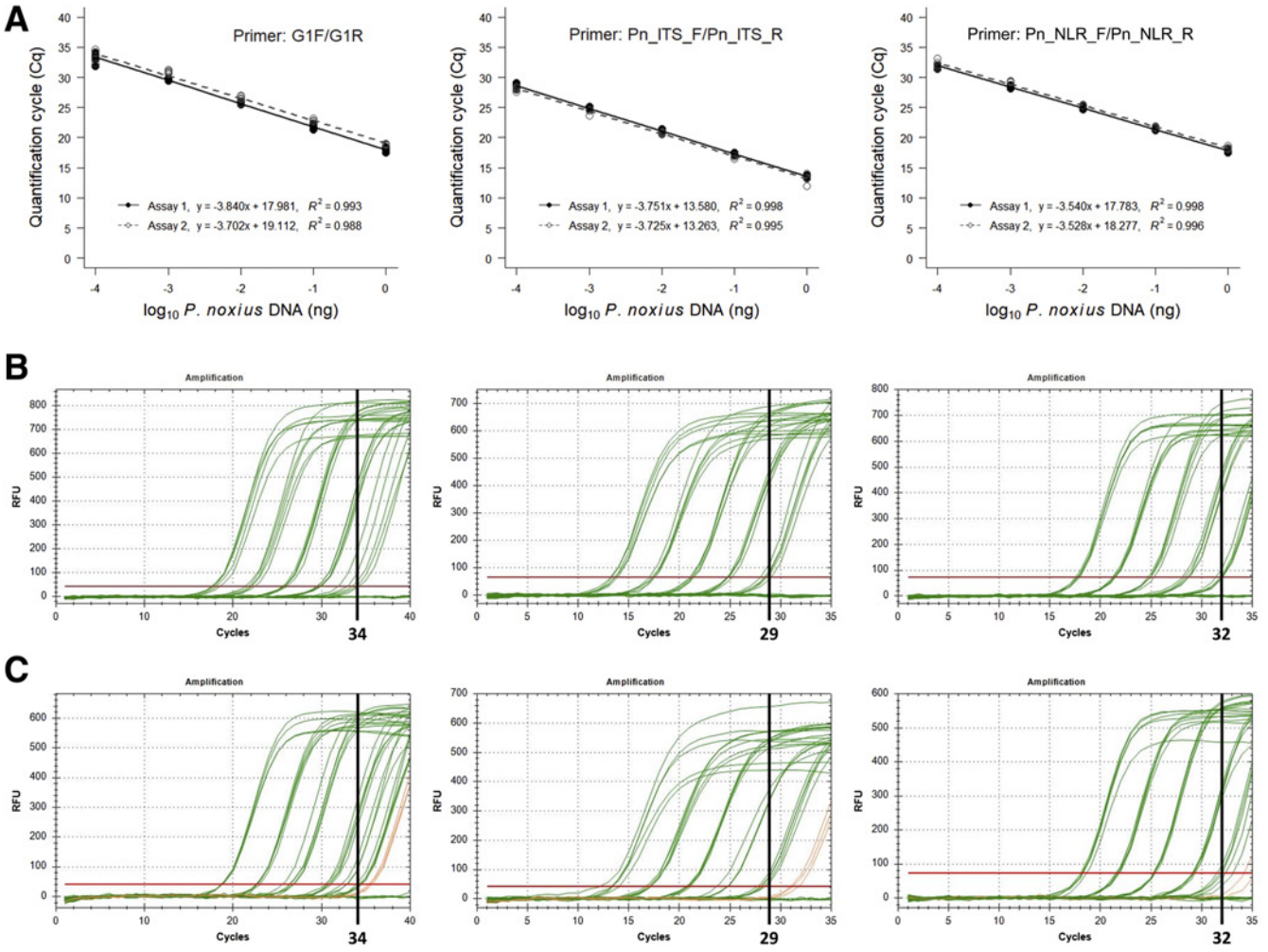

Fig. 2. Evaluation of the sensitivity of quantitative real-time PCR assays using three primer pairs. **A,** The standard curves for 10-fold serial dilutions of *Phellinus noxius* DNA (Assay 1) and for 10-fold serial dilutions of *P. noxius* DNA mixed with 50 ng of *Ficus benjamina* DNA (Assay 2). **B,** The amplification plots of Assay 1. **C,** The amplification plots of Assay 2. The black line indicates the cutoff of Cq value and the lighter (orange in the online version) amplification curves are the nonspecific signals against the DNA of *F. benjamina* (negative control). The figures in the left, middle, and right represent the results of the primer pairs G1F/G1R, Pn_ITS_F/Pn_ITS_R, and Pn_NLR_F/Pn_NLR_R, respectively. RFU = relative fluorescence units.

Table 2. Specificity tests of quantitative PCR assays

No.	Species	Isolate ID (BCRC no.)[a]	G1F/G1R		Pn_ITS_F/Pn_ITS_R		Pn_NLR_F/Pn_NLR_R	
			Cq mean ± SD[b]	Tm (°C)[c]	Cq mean ± SD[b]	Tm (°C)[c]	Cq mean ± SD[b]	Tm (°C)[c]
1	*Phellinus noxius*	CUPN026	24.2 ± 0.3	82.0	23.7 ± 0.3	82.0	22.7 ± 0.2	80.0
2	*P. noxius*	CUPN043	21.1 ± 0.3	82.0	20.2 ± 0.3	82.0	19.3 ± 0.1	79.5
3	*P. noxius*	CUPN099	19.5 ± 0.5	82.5	16.0 ± 0.1	82.0	18.1 ± 0.2	80.0
4	*P. noxius*	CUPN145	20.7 ± 0.2	82.0	16.3 ± 0.0	82.0	18.5 ± 0.1	79.5
5	*P. noxius*	CUPN167	21.3 ± 0.1	82.5	17.8 ± 0.6	82.0	19.4 ± 0.1	79.5
6	*P. noxius*	SBR	19.4 ± 0.1	82.5	18.5 ± 0.2	82.0	17.4 ± 0.1	79.5
7	*P. noxius*	JCHS	22.0 ± 0.1	82.5	16.7 ± 0.2	82.0	18.2 ± 0.1	79.0
8	*P. noxius*	E13	21.0 ± 0.2	82.5	16.6 ± 0.2	82.0	18.1 ± 0.2	80.0
9	*P. noxius*	CSG	19.6 ± 0.2	82.5	15.6 ± 0.2	82.0	17.2 ± 0.1	80.0
10	*P. noxius*	Yap 5A	21.3 ± 0.4	82.5	16.6 ± 0.1	82.0	20.8 ± 0.2	80.0
11	*P. noxius*	P919-02W.7	21.7 ± 0.1	82.5	19.6 ± 0.2	82.0	21.1 ± 0.1	80.0
12	*P. noxius*	P919-08W.4	20.4 ± 0.1	82.5	16.2 ± 0.0	82.0	20.2 ± 0.0	80.0
13	*P. noxius*	Palau 31P	22.4 ± 0.1	82.5	19.5 ± 0.6	82.0	17.9 ± 0.2	80.0
14	*P. noxius*	Palau 20P	25.2 ± 0.1	82.5	22.8 ± 0.4	82.0	21.1 ± 0.1	79.5
15	*P. noxius*	Palau 28P	22.0 ± 0.1	82.5	20.0 ± 0.3	82.0	18.1 ± 0.2	79.5
16	*P. noxius*	Palau 33P	28.0 ± 0.2	82.5	22.2 ± 0.8	82.0	18.6 ± 0.2	80.0
17	*P. noxius*	AusPn-1	22.0 ± 0.1	82.5	20.2 ± 0.1	82.0	22.3 ± 0.2	81.0
18	*P. noxius*	AusPn-6	21.3 ± 0.1	82.5	19.7 ± 0.4	82.0	20.1 ± 0.1	80.0
19	*P. noxius*	AS-1.1-PN	24.8 ± 0.1	82.5	24.0 ± 0.3	82.0	20.1 ± 0.1	79.5
20	*P. noxius*	AS-1.2-PN	24.3 ± 0.3	82.5	19.7 ± 0.3	82.0	21.6 ± 0.1	80.0
21	*P. noxius*	AS-2A.2-PN	19.7 ± 0.1	82.5	15.5 ± 0.2	82.0	18.4 ± 0.1	80.0
22	*P. noxius*	AS-2B.1-PN	19.4 ± 0.2	82.5	18.8 ± 0.4	82.0	17.8 ± 0.1	79.5
23	*P. noxius*	AS-2B.2-PN	20.6 ± 0.1	82.5	20.7 ± 0.4	82.0	18.8 ± 0.2	79.5
24	*P. noxius*	AS-3A.1-PN	23.5 ± 0.2	82.5	18.9 ± 0.5	82.0	20.3 ± 0.2	80.0
25	*P. noxius*	AS-3B.1-PN	22.3 ± 0.1	82.5	17.3 ± 0.2	81.5	20.4 ± 0.1	80.0
26	*P. noxius*	AS-3B.2-PN	19.0 ± 0.2	82.5	18.5 ± 0.5	82.0	17.5 ± 0.1	79.5
27	*P. noxius*	AS-4.1-PN	19.4 ± 0.1	82.5	14.9 ± 0.4	82.0	18.6 ± 0.3	80.0
28	*P. noxius*	AS-4.2-PN	19.2 ± 0.2	82.5	13.6 ± 0.2	82.0	20.4 ± 0.2	78.5
29	*P. noxius*	AS-4B.1-PN	20.3 ± 0.3	82.5	15.6 ± 0.4	82.0	19.4 ± 0.2	81.0
30	*P. noxius*	AS-5A.1-PN	20.9 ± 0.2	82.5	16.0 ± 0.4	82.0	19.7 ± 0.2	81.0
31	*P. noxius*	AS-5B.2-PN	21.4 ± 0.2	82.5	16.5 ± 0.3	82.0	20.3 ± 0.0	81.0
32	*P. noxius*	AS-7.1B-PN	22.4 ± 0.2	82.5	21.2 ± 0.4	82.0	19.0 ± 0.2	80.5
33	*P. noxius*	AS-8.1A-PN	19.9 ± 0.3	82.5	18.8 ± 0.1	82.0	20.1 ± 0.2	78.5
34	*P. noxius*	AS-8.1B-PN	20.0 ± 0.2	82.5	18.9 ± 0.1	82.0	20.0 ± 0.1	78.5
35	*P. noxius*	AS-13.1-PN	20.2 ± 0.1	82.5	16.3 ± 0.1	82.0	18.7 ± 0.1	80.0
36	*P. noxius*	KPN180	18.8 ± 0.1	82.5	18.5 ± 0.1	82.0	20.2 ± 0.2	79.5
37	*P. noxius*	ROTA 8B	20.0 ± 0.2	82.5	19.3 ± 0.3	82.0	19.2 ± 0.0	79.5
38	*P. noxius*	UOG3	21.8 ± 0.1	82.5	19.9 ± 0.1	82.0	20.4 ± 0.1	80.0
39	*P. noxius*	UOG17	21.4 ± 0.1	82.5	19.9 ± 0.3	82.0	20.5 ± 0.2	80.0
40	*P. noxius*	FRIM 147	20.3 ± 0.1	82.5	18.1 ± 0.4	82.0	19.0 ± 0.2	79.5
41	*P. noxius*	FRIM 557	21.2 ± 0.1	82.5	17.0 ± 0.2	82.0	18.5 ± 0.1	79.5
42	*P. noxius*	FRIM 616	20.7 ± 0.3	82.0	17.0 ± 0.1	82.0	18.0 ± 0.1	79.5
43	*P. noxius*	FRIM 620	20.5 ± 0.1	82.5	19.8 ± 0.1	82.0	19.2 ± 0.2	79.0
44	*P. noxius*	FRIM 627	22.2 ± 0.2	82.5	20.7 ± 0.3	82.0	21.5 ± 0.2	79.5
45	*P. noxius*	FRIM 727	18.4 ± 0.1	82.5	18.1 ± 0.2	82.0	18.7 ± 0.2	79.5
46	*P. noxius*	A42	19.3 ± 0.1	82.5	18.5 ± 0.4	82.0	18.5 ± 0.0	79.0
47	*P. noxius*	2252	19.0 ± 0.1	82.5	17.3 ± 0.2	82.0	16.3 ± 0.1	79.5
48	*P. noxius*	R2305	19.3 ± 0.1	82.5	16.5 ± 0.1	82.0	19.1 ± 0.1	79.5
49	*P. noxius*	R2309	17.9 ± 0.1	82.5	17.8 ± 0.4	82.0	17.7 ± 0.1	80.0
50	*P. noxius*	R2530	19.3 ± 0.1	82.5	15.1 ± 0.1	82.0	17.5 ± 0.1	79.5
51	*P. noxius*	R29342	19.3 ± 0.1	82.0	16.4 ± 0.1	82.0	17.3 ± 0.1	80.0
52	*P. noxius*	R29369	21.6 ± 0.1	82.5	21.5 ± 0.0	82.0	25.2 ± 0.0	80.5
53	*P. noxius*	R210205	19.2 ± 0.1	82.0	17.4 ± 0.2	82.0	17.5 ± 0.2	79.5
54	*P. noxius*	TPI-B2-9	19.6 ± 0.1	82.0	16.6 ± 0.1	81.5	18.3 ± 0.1	79.0
55	*P. noxius*	2248	22.3 ± 0.2	82.5	17.0 ± 0.4	82.0	19.5 ± 0.2	79.5
56	*P. noxius*	B98	22.1 ± 0.1	82.5	18.6 ± 0.4	82.0	17.4 ± 0.0	79.5
57	*P. noxius*	TFRI 818 (BCRC 35248)	18.5 ± 0.6	82.0	20.5 ± 0.7	82.0	19.2 ± 1.0	79.5
58	*P. noxius*	TFRI 826 (BCRC 35249)	18.5 ± 0.4	82.0	20.6 ± 0.8	82.0	18.3 ± 1.1	80.0
59	*P. noxius*	TFRI 828 (BCRC 35250)	17.1 ± 0.4	82.0	18.7 ± 0.4	82.0	18.5 ± 1.1	80.0
60	*P. noxius*	TFRI 22 (BCRC 35252)	18.2 ± 0.1	82.5	15.8 ± 0.3	82.0	19.3 ± 1.1	79.0
61	*P. noxius*	TFRI 566 (BCRC 35436)	20.1 ± 0.1	82.5	18.4 ± 0.2	80.0	19.6 ± 1.1	80.0
62	*P. apiahynus*	TFRI 34 (BCRC 35468)	–	–	–	–	34.6 ± 2.7	79.5
63	*P. hoehnelii*	TFRI 500 (BCRC 35424)	–	–	–	–	–	–

(*Continued on next page*)

[a] BCRC = Bioresource Collection and Research Center; TFRI = Taiwan Forestry Research Institute.
[b] Cq = quantification of cycle. Cq mean ± SD is the mean of three replications with its SD. "–" indicates no amplification.
[c] Tm = melting temperature.

Table 2. (*Continued from previous page*)

No.	Species	Isolate ID (BCRC no.)[a]	G1F/G1R		Pn_ITS_F/Pn_ITS_R		Pn_NLR_F/Pn_NLR_R	
			Cq mean ± SD[b]	Tm (°C)[c]	Cq mean ± SD[b]	Tm (°C)[c]	Cq mean ± SD[b]	Tm (°C)[c]
64	*P. igniarius*	TFRI 213 (BCRC 35308)	–	–	–	–	–	–
65	*P. laevigatus*	TFRI 634 (BCRC 35495)	–	–	–	–	–	–
66	*P. quercinus*	TFRI 254 (BCRC 35352)	–	–	–	–	–	–
67	*Antrodia cinnamomea*	TFRI 119 (BCRC 35396)	–	–	–	–	–	–
68	*Coriolopsis aspera*	TFRI 118 (BCRC 35323)	25.0 ± 0.6	85.0	–	–	–	–
69	*Earliella scabrosa*	TFRI 29 (BCRC 35254)	–	–	35.3 ± 1.5	82.0	–	–
70	*Ganoderma australe*	TFRI 17 (BCRC 35394)	–	–	–	–	–	–
71	*G. australe*	TFRI 03 (BCRC 35400)	–	–	–	–	–	–
72	*G. boninense*	TFRI 129 (BCRC 35348)	–	–	–	–	–	–
73	*G. fornicatum*	TFRI 396 (BCRC 35374)	37.5 ± 0.7	80.5	–	–	–	–
74	*G. limushanense*	TFRI 58 (BCRC 35295)	–	–	–	–	–	–
75	*G. lucidum*	TFRI 80 (BCRC 35412)	–	–	–	–	–	–
76	*G. weberianum*	TFRI 121 (BCRC 35401)	–	–	–	–	–	–
77	*Heterobasidion annosum*	TFRI 672 (BCRC 35493)	–	–	–	–	–	–
78	*Polyporus arcularius*	TFRI 284 (BCRC 35355)	–	–	–	–	–	–
79	*P. badius*	TFRI 542 (BCRC 35461)	–	–	–	–	–	–
80	*P. brumalis*	TFRI 561 (BCRC 35439)	–	–	–	–	–	–
81	*P. ciliatus*	TFRI 458 (BCRC 35391)	–	–	–	–	–	–
82	*P. squamosus*	TFRI 23 (BCRC 35319)	–	–	–	–	–	–
83	*P. varius*	TFRI 582 (BCRC 35471)	–	–	–	–	–	–
84	*Pycnoporus sanguineus*	TFRI 70 (BCRC 35298)	–	–	37.1 ± 0.4	82.0	–	–
85	*Rigidoporus lineatus*	TFRI 20 (BCRC 35318)	–	–	–	–	–	–
86	*Rigidoporus ulmarius*	TFRI 537 (BCRC 35460)	–	–	36.1 ± 0.8	80.0	35.1 ± 0.1	80.0
87	*Schizophyllum commune*	TFRI 255 (BCRC 35328)	–	–	36.5 ± 1.5	79.0	33.7 ± 0.7	79.0
88	*Trametes versicolor*	TFRI 31 (BCRC 35253)	–	–	–	–	–	–
89	*Xylobolus subpileatus*	TFRI 258 (BCRC 35329)	–	–	–	–	–	–

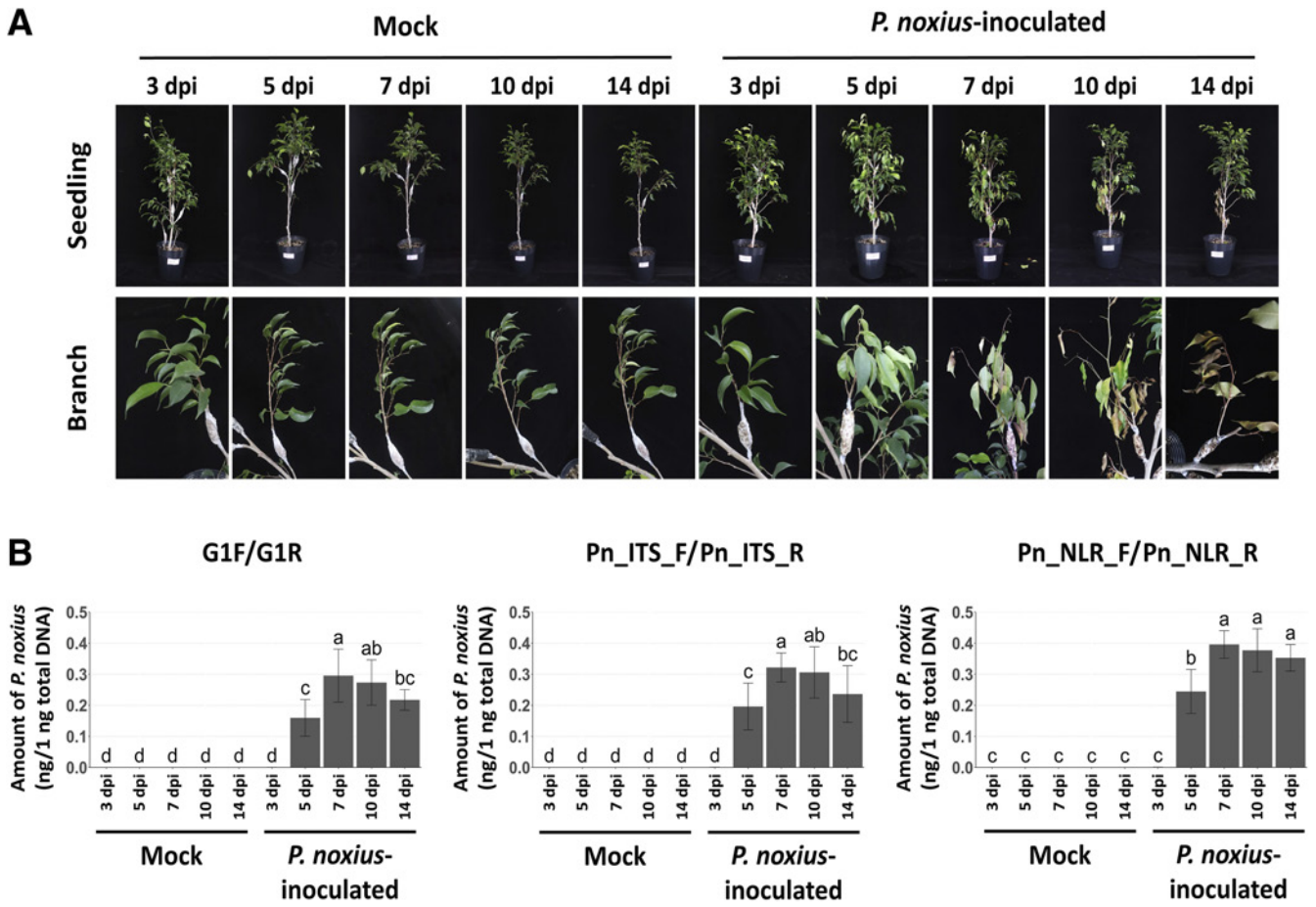

Fig. 3. Evaluation of the amounts of *Phellinus noxius* in inoculated *Ficus benjamina* tissues by quantitative real-time PCR (qPCR) assays. **A,** Two-year-old *F. benjamina* seedlings were inoculated with *P. noxius*–colonized grains on wounded branches. Photos were taken at 3, 5, 7, 10, and 14 days postinoculation (dpi). Mock inoculation represents the inoculation with sterile grains. **B,** The amounts of *P. noxius* were determined by qPCR using three primer pairs: G1F/G1R, Pn_ITS_F/Pn_ITS_R, and Pn_NLR_F/Pn_NLR_R. Data (mean ± SD) with different letters are significantly different according to Tukey's honestly significant difference test at $P < 0.05$.

these genes of *P. noxius*. The sequences of nuclear large subunit, partial RNA polymerase II, and partial translation elongation factor 1-alpha have been used for phylogenetic and population genetic analyses of *P. noxius* (Stewart et al. 2020), but the variation in these genes among *P. noxius* and other *Phellinus* spp. is not sufficient for developing *P. noxius*–specific target sequences. In this study, through a comparative analysis of 61 fungal genomes, we identified a *P. noxius*–unique group of genes belonging to the NLR superfamily and designed *P. noxius*–specific primers Pn_NLR_F/Pn_NLR_R suitable for qPCR. The NLR superfamily exhibits high diversity within fungi and has been associated with programmed cell death, vegetative incompatibility, and nonself recognition (Bidard et al. 2013). A high copy number and extensive diversity of the NLR superfamily has been previously reported for *P. noxius* (Chung et al. 2017). Indeed, as many as 84 homologous genes belonging to the unique group were identified in the genome of *P. noxius* FFPRI411160; many SNPs exist among NLR sequences of the same or different *P. noxius* isolates. As a template for PCR amplification, the high copy number characteristics of both ITS and NLR sequences are advantageous for higher sensitivity. Additionally, the slightly different Tm of each primer pair may be related to the SNPs and indels in the amplicons of different *P. noxius* isolates.

Typically, the accepted range for qPCR efficiency is 90 to 110% (Bustin et al. 2009). To ensure sufficient specificity, the optimal annealing/extension temperatures were determined to be 65°C for G1F/G1R and Pn_NLR_F/Pn_NLR_R and 68°C for Pn_ITS_F/Pn_

Table 3. Quantitative PCR detection of *Phellinus noxius* in tree roots and soil samples

Location	Tree species	Sample ID[a]	Sample type	Symptoms or sign[b]	*P. noxius* isolation[c]	qPCR result (Cq mean ± SD)[d]		
						G1F/G1R[e]	Pn_ITS_F/ Pn_ITS_R	Pn_NLR_F/ Pn_NLR_R
National Taiwan University	*Salix babylonica*	A1	Root tissue	W	+	+ (26.6 ± 0.4)	+ (24.0 ± 0.3)	+ (25.8 ± 0.2)
		A2	Root tissue	–	–	– (34.4 ± 1.5)	– (32.8 ± 1.1)	– (34.1 ± 0.7)
		A3	Root tissue	–	–	– (37.8 ± 1.9)	– (34.7 ± 0.6)	– (37.6)
		A4	Root tissue	–	–	– (35.1 ± 0.2)	– (0.0)	– (38.8)
		A1_BS	Bulk soil around A1	–	N.T.	– (37.8)	– (0.0)	– (0.0)
		A2_BS	Bulk soil around A2	–	N.T.	– (0.0)	– (34.7)	– (0.0)
		A3_BS	Bulk soil around A3	–	N.T.	– (0.0)	– (0.0)	– (0.0)
		A4_BS	Bulk soil around A4	–	N.T.	– (0.0)	– (0.0)	– (38.3)
	Salix babylonica	B1	Root tissue	Y, W, H	–	– (38.2 ± 1.1)	– (35.4 ± 2.1)	– (34.9 ± 0.4)
		B2	Root tissue	Y, W, H	+	+ (22.1 ± 0.2)	+ (19.7 ± 0.1)	+ (22.7 ± 0.2)
		B3	Root tissue	Y, W, H	+	+ (21.6 ± 0.3)	+ (18.6 ± 0.1)	+ (21.4 ± 0.1)
		B4	Root tissue	Y, W, H	+	+ (18.3 ± 0.1)	+ (16.2 ± 0.2)	+ (19.2 ± 0.1)
		B1_BS	Bulk soil around B1	–	N.T.	– (39.2 ± 0.3)	– (39.3)	– (0.0)
		B2_BS	Bulk soil around B2	–	N.T.	– (0.0)	– (34.4 ± 0.3)	– (37.5 ± 0.7)
		B3_BS	Bulk soil around B3	–	N.T.	– (36.7 ± 1.5)	– (34.8 ± 0.9)	– (34.5 ± 2.1)
		B4_BS	Bulk soil around B4	–	N.T.	– (0.0)	– (34.4 ± 0.4)	– (35.9 ± 1.0)
	Camphora officinarum	C1	Root tissue	Y, W	+	+ (18.7 ± 0.4)	+ (16.1 ± 1.0)	+ (17.0 ± 1.1)
		C2	Root tissue	Y, W	+	+ (17.2 ± 0.3)	+ (14.5 ± 0.9)	+ (17.2 ± 0.2)
		C3	Root tissue	Y, W	+	+ (18.2 ± 0.2)	+ (15.5 ± 0.5)	+ (18.2 ± 0.1)
		C4	Root tissue	Y, W	+	+ (22.9 ± 0.2)	+ (20.2 ± 0.2)	+ (23.3 ± 0.0)
		C1_RS	Rhizosphere soil around C1	–	N.T.	+ (24.2 ± 0.1)	+ (21.4 ± 0.4)	+ (25.7 ± 0.0)
		C2_RS	Rhizosphere soil around C2	–	N.T.	+ (21.8 ± 0.2)	+ (18.8 ± 0.2)	+ (23.2 ± 0.0)
		C3_RS	Rhizosphere soil around C3	–	N.T.	+ (26.6 ± 0.2)	+ (24.2 ± 0.0)	+ (27.7 ± 0.2)
		C4_RS	Rhizosphere soil around C4	–	N.T.	+ (26.1 ± 0.2)	+ (23.7 ± 0.3)	+ (27.2 ± 0.1)
		C1_BS	Bulk soil around C1	–	N.T.	+ (30.7 ± 0.4)	+ (28.2 ± 0.1)	+ (30.5 ± 0.1)
		C2_BS	Bulk soil around C2	–	N.T.	– (35.0 ± 0.6)	– (35.0 ± 0.7)	– (35.8 ± 0.5)
		C3_BS	Bulk soil around C3	–	N.T.	– (35.9 ± 0.5)	– (37.1 ± 3.6)	– (37.5 ± 1.9)
		C4_BS	Bulk soil around C4	–	N.T.	– (36.0 ± 1.5)	– (0.0)	– (0.0)
	Salix babylonica	N1	Branch tissue	–	–	– (0.0)	– (0.0)	– (0.0)
		N2	Branch tissue	–	–	– (0.0)	– (0.0)	– (0.0)
	Camphora officinarum	O1	Branch tissue	–	–	– (0.0)	– (0.0)	– (0.0)
		O2	Branch tissue	–	–	– (0.0)	– (0.0)	– (0.0)
Feitsui Reservoir	*Ficus microcarpa*	D1	Root tissue	M, W, H	N.T.	+ (19.2 ± 0.2)	+ (17.7 ± 0.1)	+ (15.8 ± 0.3)
		D2	Root tissue	M, W, H	N.T.	+ (24.0 ± 0.2)	+ (22.3 ± 0.1)	+ (20.8 ± 0.1)
		D3	Root tissue	M, W, H	N.T.	+ (21.6 ± 0.1)	+ (19.9 ± 0.1)	+ (18.1 ± 0.2)
		D4	Root tissue	M, W, H	N.T.	– (34.7 ± 0.7)	– (31.4 ± 0.4)	+ (31.3 ± 0.6)
	Ficus microcarpa	E1	Root tissue	M, W, H	+	+ (23.1 ± 0.1)	+ (21.8 ± 0.2)	+ (19.9 ± 0.1)
		E2	Root tissue	M, W, H	+	+ (22.5 ± 0.1)	+ (21.0 ± 0.1)	+ (19.4 ± 0.2)
		E3	Root tissue	M, W, H	+	+ (22.8 ± 0.2)	+ (21.7 ± 0.2)	+ (19.3 ± 0.2)
		E4	Root tissue	M, W, H	+	+ (22.4 ± 0.5)	+ (20.8 ± 0.1)	+ (18.6 ± 0.2)

(*Continued on next page*)

[a] A to P indicates 17 trees. "A and B" and "D and E" and "F and G" were neighboring trees at the same infection site. The numbers 1 to 4 indicate the samples collected from different sites around a tree. NTC = no template control.

[b] H = brown to reddish hyphal strands on decayed wood tissues; M = brown to black mycelial mat; W = white-rotted wood tissues; Y = yellowing and wilting of leaves. "–" indicates no symptom/sign or not applicable.

[c] Tissue isolation was conducted to detect viable *P. noxius* in root tissues. "+" indicates *P. noxius* was isolated. "–" indicates *P. noxius* was not isolated. N.T. = not tested.

[d] Cq = Quantification of cycle. Cq mean ± SD is the mean of three replications with its SD. "+" indicates the detection of *P. noxius*. "–" indicates no detection. The cutoff Cq values were 34 for G1F/G1R, 29 for Pn_ITS_F/Pn_ITS_R, and 32 for Pn_NLR_F/Pn_NLR_R.

[e] Primer pairs are described in Table 1.

[f] ddH_2O = double-distilled water.

ITS_R. As the annealing temperature increases, the sensitivity and efficiency of the qPCR assay decrease. Pn_NLR_F/Pn_NLR_R exhibited a high efficiency of 95.8%, whereas G1F/G1R and Pn_ITS_F/Pn_ITS_R exhibited an efficiency of ca. 83%, below 90%. The lower efficiency of G1F/G1R and Pn_ITS_F/Pn_ITS_R may be attributed to the larger size of their amplicons (Table 1) (Suárez et al. 2022). The R^2 values for qPCR standard curves were >0.99, indicating that pipetting was not the source of lower efficiency values. During the primer development stage, we designed and tested many ITS-based primer pairs with amplicon sizes in the generally recommended range (90 to 300 bp), but none of them had good specificity. Despite the difference in efficiency, all three primer pairs could detect as little as 100 fg of *P. noxius* genomic DNA, demonstrating a sensitivity 100 times higher than that of conventional PCR (Wu et al. 2009).

When performing qPCR assays, including a negative control (healthy plant tissue) and adopting the cutoff Cq value are critical for accurate interpretation of the results. For all three primer pairs, occasional nonspecific signals with high Cq values were detected from other fungi and host plants (e.g., *F. microcarpa* DNA at higher concentration [50 ng per reaction]; no nonspecific signals were detected when using 10 ng DNA per reaction). The false-positive results could be avoided by applying the cutoff Cq value corresponding to the LOD (Caraguel et al. 2011; Grosdidier et al. 2017). This approach has been employed to ensure the accuracy of the diagnostic assays for other plant pathogens, such as *Ilyonectria robusta*, *Peronospora destructor*, *Pectobacterium carotovorum*, *Ramularia mali*, and *Xanthomonas fragariae* (Fujiwara et al. 2021; Jiang et al. 2023; Prencipe et al. 2023; Suárez et al. 2022; Turechek and Wang 2023). Because *P. noxius* mainly infects the roots and stem base of trees, and because symptoms and signs may not be observed at the early stages of BRRD, a branch sample from the tested tree can serve as a negative control.

The new qPCR assays were used for quantifying *P. noxius* DNA in infected tissues of seven tree species. To simplify inoculation and sampling, we developed the method for inoculating branches of *F. benjamina* seedlings with *P. noxius*–colonized grains. Based on the results from all three primer pairs, *P. noxius* DNA increased in inoculated branches from 3 to 7 dpi, corresponding to the observed increasing BRRD severity. Although the wilting symptom became more severe from 7 to 14 dpi, the detected amount of *P. noxius* DNA did not increase during this time period. At the late stage of BRRD development, DNA extracted from decomposed tissues may be of lower quality and thus affect the quantification results (Ikeda et al. 2008). When testing field samples by qPCR, we found that the amounts of *P. noxius* DNA in different samples from the same diseased tree varied greatly. Because mature trees have extensive root systems and *P. noxius* infection is not evenly distributed, sampling from multiple sites around the tree is recommended to reduce the false negatives.

In conclusion, new qPCR assays based on the ITS and NLR regions of *P. noxius* were developed, and the utility for *P. noxius* detection was evaluated. Owing to the occasional detection of nonspecific signals, it is crucial to apply the cutoff Cq values (34 for G1F/G1R, 29 for Pn_ITS_F/Pn_ITS_R, and 32 for Pn_NLR_F/Pn_NLR_R) to avoid any false positives. The qPCR assays can be used as a first step in identifying symptomless trees that are infected with *P. noxius*. It should be noted that qPCR assays do not determine the viability of the pathogen. Survival of *P. noxius* is mainly within diseased tree stumps, roots, and wood debris, and no viable *P. noxius* was recovered from the soil, even from the rhizosphere soil around the symptomatic diseased roots (Wu et al. 2020). Consistent with previous findings (Wang et al. 2016; Wu et al. 2020), we detected *P. noxius* DNA from the rhizosphere soil and bulk soil samples. The presence of *P. noxius* DNA in the soil can be attributed to dead pathogens or pathogen DNA released from diseased roots (Whitchurch et al. 2002).

Table 3. (*Continued from previous page*)

Location	Tree species	Sample ID[a]	Sample type	Symptoms or sign[b]	*P. noxius* isolation[c]	qPCR result (Cq mean ± SD)[d]		
						G1F/G1R[e]	Pn_ITS_F/ Pn_ITS_R	Pn_NLR_F/ Pn_NLR_R
Taipei Botanical Garden	*Ficus microcarpa*	F1	Root tissue	M, H	+	+ (23.6 ± 0.3)	+ (24.0 ± 0.1)	+ (19.6 ± 0.2)
		F2	Root tissue	M, H	+	+ (22.7 ± 0.1)	+ (23.5 ± 0.3)	+ (18.9 ± 0.1)
		F3	Root tissue	M, H	+	+ (23.9 ± 0.3)	+ (24.5 ± 0.2)	+ (20.2 ± 0.2)
		F4	Root tissue	M, H	+	+ (25.7 ± 0.4)	+ (21.5 ± 0.3)	+ (25.6 ± 0.2)
	Ficus microcarpa	G1	Root tissue	M, H	+	+ (21.2 ± 0.2)	+ (17.1 ± 0.1)	+ (22.4 ± 0.1)
		G2	Root tissue	M, H	+	+ (21.6 ± 0.3)	+ (17.5 ± 0.3)	+ (22.5 ± 0.1)
		G3	Root tissue	M, H	+	+ (20.0 ± 0.0)	+ (15.8 ± 0.2)	+ (21.0 ± 0.1)
		G4	Root tissue	M, H	+	+ (20.1 ± 0.0)	+ (16.0 ± 0.1)	+ (21.4 ± 0.1)
	Bischofia javanica	H1	Root tissue	W	+	+ (21.7 ± 0.1)	+ (17.5 ± 0.1)	+ (22.4 ± 0.0)
		H2	Root tissue	W	+	+ (27.6 ± 0.2)	+ (23.1 ± 0.3)	+ (27.7 ± 0.2)
		H3	Root tissue	W	+	+ (24.1 ± 0.2)	+ (19.9 ± 0.1)	+ (24.7 ± 0.2)
		H4	Root tissue	W	+	+ (22.9 ± 0.4)	+ (18.6 ± 0.2)	+ (23.4 ± 0.2)
	Koelreuteria elegans	I1	Root tissue	W	+	+ (30.5 ± 0.4)	+ (26.5 ± 0.3)	+ (28.2 ± 0.4)
		I2	Root tissue	W	+	+ (34.0 ± 0.4)	+ (28.3 ± 0.1)	+ (30.8 ± 0.6)
		I3	Root tissue	W	+	+ (27.3 ± 0.2)	+ (22.2 ± 0.1)	+ (24.9 ± 0.1)
		I4	Root tissue	W	+	+ (30.6 ± 0.5)	+ (26.2 ± 0.1)	+ (28.3 ± 0.1)
	Zelkova serrata	J1	Root tissue	W	+	+ (19.6 ± 0.2)	+ (16.4 ± 0.3)	+ (18.4 ± 0.1)
		J2	Root tissue	W	+	+ (18.7 ± 0.3)	+ (15.6 ± 0.1)	+ (17.5 ± 0.1)
		J3	Root tissue	W	+	+ (20.3 ± 0.1)	+ (17.3 ± 0.2)	+ (18.9 ± 0.1)
		J4	Root tissue	W	+	+ (20.1 ± 0.1)	+ (16.8 ± 0.1)	+ (18.7 ± 0.2)
	Ficus microcarpa	K1	Branch tissue	–	–	– (0.0)	– (37.6)	– (0.0)
		K2	Branch tissue	–	–	– (0.0)	– (0.0)	– (34.7 ± 1.7)
	Bischofia javanica	L1	Branch tissue	–	–	– (0.0)	– (0.0)	– (0.0)
		L2	Branch tissue	–	–	– (0.0)	– (0.0)	– (0.0)
	Koelreuteria elegans	M1	Branch tissue	–	–	– (0.0)	– (0.0)	– (0.0)
		M2	Branch tissue	–	–	– (0.0)	– (0.0)	– (0.0)
	Zelkova serrata	P1	Branch tissue	–	–	– (0.0)	– (0.0)	– (0.0)
		P2	Branch tissue	–	–	– (0.0)	– (0.0)	– (0.0)
		NTC	ddH_2O[f]	–	N.T.	– (0.0)	– (0.0)	– (0.0)

It is worth exploring whether the quantity of *P. noxius* DNA present in the rhizosphere soil can serve as a nondestructive indicator for monitoring disease development.

Acknowledgments

We thank Schung-Ching Chiu, Yu-Ching Huang, and Ashley Lehman for providing *P. noxius* isolates.

Literature Cited

Altschul, S. F., Madden, T. L., Schäffer, A. A., Zhang, J., Zhang, Z., Miller, W., and Lipman, D. J. 1997. Gapped BLAST and PSI-BLAST: A new generation of protein database search programs. Nucleic Acids Res. 25:3389-3402.

Ann, P.-J., Chang, T.-T., and Ko, W.-H. 2002. *Phellinus noxius* brown root rot of fruit and ornamental trees in Taiwan. Plant Dis. 86:820-826.

Bidard, F., Clavé, C., and Saupe, S. J. 2013. The transcriptional response to nonself in the fungus *Podospora anserina*. G3 3:1015-1030.

Broeders, S., Huber, I., Grohmann, L., Berben, G., Taverniers, I., Mazzara, M., Roosens, N., and Morisset, D. 2014. Guidelines for validation of qualitative real-time PCR methods. Trends Food Sci. Technol. 37:115-126.

Bustin, S. A., Benes, V., Garson, J. A., Hellemans, J., Huggett, J., Kubista, M., Mueller, R., Nolan, T., Pfaffl, M. W., Shipley, G. L., Vandesompele, J., and Wittwer, C. T. 2009. The MIQE guidelines: Minimum information for publication of quantitative real-time PCR experiments. Clin. Chem. 55: 611-622.

Caraguel, C. G. B., Stryhn, H., Gagné, N., Dohoo, I. R., and Hammell, K. L. 2011. Selection of a cutoff value for real-time polymerase chain reaction results to fit a diagnostic purpose: Analytical and epidemiologic approaches. J. Vet. Diagn. Invest. 23:2-15.

Chang, T.-T. 1992. Decline of some forest trees associated with brown root rot caused by *Phellinus noxius*. Plant Pathol. Bull. 1:90-95.

Chang, T.-T. 1995. A selective medium for *Phellinus noxius*. Eur. J. For. Pathol. 25:185-190.

Chang, T.-T. 1996. Survival of *Phellinus noxius* in soil and in the roots of dead host plants. Phytopathology 86:272-276.

Chen, C.-Y., Chen, S.-Y., Liu, C.-W., Wu, D.-H., Kuo, C.-C., Lin, C.-C., Chou, H.-P., Wang, Y.-Y., Tsai, Y.-C., Lai, M.-H., and Chung, C.-L. 2020. Invasion and colonization pattern of *Fusarium fujikuroi* in rice. Phytopathology 110: 1934-1945.

Chen, C.-Y., Wu, Z.-C., Liu, T.-Y., Yu, S.-S., Tsai, J.-N., Tsai, Y.-C., Tsai, I. J., and Chung, C.-L. 2023. Investigation of asymptomatic infection of *Phellinus noxius* in herbaceous plants. Phytopathology 113:460-469.

Cherubini, P., Fontana, G., Rigling, D., Dobbertin, M., Brang, P., and Innes, J. L. 2002. Tree-life history prior to death: Two fungal root pathogens affect tree-ring growth differently. J. Ecol. 90:839-850.

Chou, H., Xiao, Y.-T., Tsai, J.-N., Li, T.-T., Wu, H.-Y., Liu, L.-y. D., Tzeng, D.-S., and Chung, C.-L. 2019. In vitro and in planta evaluation of *Trichoderma asperellum* TA as a biocontrol agent against *Phellinus noxius*, the cause of brown root rot disease of trees. Plant Dis. 103:2733-2741.

Chung, C.-L., Huang, S.-Y., Huang, Y.-C., Tzean, S.-S., Ann, P.-J., Tsai, J.-N., Yang, C.-C., Lee, H.-H., Huang, T.-W., Huang, H.-Y., Chang, T.-T., Lee, H.-L., and Liou, R.-F. 2015. The genetic structure of *Phellinus noxius* and dissemination pattern of brown root rot disease in Taiwan. PLoS One 10: e0139445.

Chung, C.-L., Lee, T. J., Akiba, M., Lee, H.-H., Kuo, T.-H., Liu, D., Ke, H.-M., Yokoi, T., Roa, M. B., Lu, M.-Y. J., Chang, Y.-Y., Ann, P.-J., Tsai, J.-N., Chen, C.-Y., Tzean, S.-S., Ota, Y., Hattori, T., Sahashi, N., Liou, R.-F., Kikuchi, T., and Tsai, I. J. 2017. Comparative and population genomic landscape of *Phellinus noxius*: A hypervariable fungus causing root rot in trees. Mol. Ecol. 26:6301-6316.

Chung, P.-C., Wu, H.-Y., Chen, Y.-C., Hung, T.-H., and Chung, C.-L. 2022. Development of a nested PCR assay for detecting *Colletotrichum siamense* and *Colletotrichum fructicola* on symptomless strawberry plants. PLoS One 17:e0270687.

Davidson, R. W., Campbell, W. A., and Blaisdell, D. J. 1938. Differentiation of wood-decaying fungi by their reactions on gallic or tannic acid medium. J. Agric. Res. 57:683-695.

de Mendiburu, F. 2014. agricolae: Statistical procedures for agricultural research. R. Package Version 1. https://doi.org/10.32614/CRAN.package.agricolae

Dyrka, W., Lamacchia, M., Durrens, P., Kobe, B., Daskalov, A., Paoletti, M., Sherman, D. J., and Saupe, S. J. 2014. Diversity and variability of NOD-like receptors in fungi. Genome Biol. Evol. 6:3137-3158.

Emms, D. M., and Kelly, S. 2015. OrthoFinder: Solving fundamental biases in whole genome comparisons dramatically improves orthogroup inference accuracy. Genome Biol. 16:157.

Fatima, T., Srivastava, A., Hanur, V. S., and Rao, M. S. 2018. An effective wood DNA extraction protocol for three economic important timber species of India. Am. J. Plant Sci. 9:139-149.

Fujiwara, K., Inoue, H., Sonoda, R., Iwamoto, Y., Kusaba, M., Tashiro, N., and Miyasaka, A. 2021. Real-time PCR detection of the onion downy mildew pathogen *Peronospora destructor* from symptomless onion seedlings and soils. Plant Dis. 105:643-649.

Grosdidier, M., Aguayo, J., Marçais, B., and Ioos, R. 2017. Detection of plant pathogens using real-time PCR: How reliable are late C_t values? Plant Pathol. 66:359-367.

Hariharan, G., and Prasannath, K. 2020. Recent advances in molecular diagnostics of fungal plant pathogens: A mini review. Front. Cell. Infect. Microbiol. 10: 600234.

Hsiao, W.-W., Hung, T.-H., and Sun, E.-J. 2019. Newly discovered basidiocarps of *Phellinus noxius* on 33 tree species with brown root rot disease in Taiwan and the basidiospore variations in growth rate. Taiwania 64:263-268.

Huang, Y. H., Chen, C. H., Hung, T. H., Wu, M. L., and Chang, T. T. 2014. Development of the detection method for tree brown root rot disease based on the loop-mediated isothermal amplification (LAMP). Plant Pathol. Bull. 23:1-13.

Ikeda, S., Tsurumaru, H., Wakai, S., Noritake, C., Fujishiro, K., Akasaka, M., and Ando, K. 2008. Evaluation of the effects of different additives in improving the DNA extraction yield and quality from andosol. Microbes Environ. 23: 159-166.

Inglis, P. W., Pappas, M. d. C. R., Resende, L. V., and Grattapaglia, D. 2018. Fast and inexpensive protocols for consistent extraction of high quality DNA and RNA from challenging plant and fungal samples for high-throughput SNP genotyping and sequencing applications. PLoS One 13:e0206085.

Jiang, Y., Jin, H., Li, X., Yan, D., Zhang, Y., Li, M., Gao, J., Lu, B., Chen, C., and Jiang, Y. 2023. Development of a novel real-time quantitative PCR method for detection of *Ilyonectria robusta*, the predominant species causing ginseng rusty root rot. Plant Dis. 107:1680-1689.

Katoh, K., Misawa, K., Kuma, K.-i., and Miyata, T. 2002. MAFFT: A novel method for rapid multiple sequence alignment based on fast Fourier transform. Nucleic Acids Res. 30:3059-3066.

Katoh, K., Rozewicki, J., and Yamada, K. D. 2019. MAFFT online service: Multiple sequence alignment, interactive sequence choice and visualization. Brief. Bioinform. 20:1160-1166.

Kozhar, O., Kim, M.-S., Ibarra Caballero, J., Klopfenstein, N. B., Cannon, P. G., and Stewart, J. E. 2022. Long evolutionary history of an emerging fungal pathogen of diverse tree species in eastern Asia, Australia and the Pacific Islands. Mol. Ecol. 31:2013-2031.

Leung, K.-T., Chen, C.-Y., You, B.-J., Lee, M.-H., and Huang, J.-W. 2020. Brown root rot disease of *Phyllanthus myrtifolius*: The causal agent and two potential biological control agents. Plant Dis. 104:3043-3053.

Liao, T.-Z., Chen, Y.-H., Tsai, J.-N., Chao, C., Huang, T.-P., Hong, C.-F., Wu, Z.-C., Tsai, I. J., Lee, H.-H., Klopfenstein, N. B., Kim, M.-S., Stewart, J. E., Atibalentja, N., Brooks, F. E., Cannon, P. G., Farid, A. M., Hattori, T., Kwan, H.-S., Ching Lam, R. Y., Ota, Y., Sahashi, N., Schlub, R. L., Shuey, L. S., Tang, A. M. C., and Chung, C.-L. 2023. Translocation of fungicides and their efficacy in controlling *Phellinus noxius*, the cause of brown root rot disease. Plant Dis. 107:2039-2053.

Liu, T.-Y., Chen, C.-H., Yang, Y.-L., Tsai, I. J., Ho, Y.-N., and Chung, C.-L. 2022. The brown root rot fungus *Phellinus noxius* affects microbial communities in different root-associated niches of *Ficus* trees. Environ. Microbiol. 24:276-297.

McCartney, H. A., Foster, S. J., Fraaije, B. A., and Ward, E. 2003. Molecular diagnostics for fungal plant pathogens. Pest Manag. Sci. 59:129-142.

Prencipe, S., Valente, S., Nari, L., and Spadaro, D. 2023. A quantitative real-time PCR assay for early detection and quantification of *Ramularia mali*, an emerging pathogen of apple causing dry lenticel rot. Plant Dis. 107:1399-1407.

Proell, M., Riedl, S. J., Fritz, J. H., Rojas, A. M., and Schwarzenbacher, R. 2008. The nod-like receptor (NLR) family: A tale of similarities and differences. PLoS One 3:e2119.

Schoch, C. L., Seifert, K. A., Huhndorf, S., Robert, V., Spouge, J. L., Levesque, C. A., Chen, W., Fungal Barcoding Consortium, Bolchacova, E., Voigt, K., Crous, P. W., Miller, A. N., Wingfield, M. J., Aime, M. C., An, K.-D., Bai, F.-Y., Barreto, R. W., Begerow, D., Bergeron, M.-J., Blackwell, M., Boekhout, T., Bogale, M., Boonyuen, N., Burgaz, A. R., Buyck, B., Cai, L., Cai, Q., Cardinali, G., Chaverri, P., Coppins, B. J., Crespo, A., Cubas, P., Cummings, C., Damm, U., de Beer, Z. W., de Hoog, G. S., Del-Prado, R., Dentinger, B., Diéguez-Uribeondo, J., et al. 2012. Nuclear ribosomal internal transcribed spacer (ITS) region as a universal DNA barcode marker for *Fungi*. Proc. Natl. Acad. Sci. U.S.A. 109:6241-6246.

Stewart, J. E., Kim, M.-S., Ota, Y., Sahashi, N., Hanna, J. W., Akiba, M., Ata, J. P., Atibalentja, N., Brooks, F., Chung, C.-L., Dann, E. K., Mohd Farid, A., Hattori, T., Lee, S. S., Otto, K., Pegg, G. S., Schlub, R. L., Shuey, L. S., Tang, A. M. C., Tsai, J.-N., Cannon, P. G., and Klopfenstein, N. B. 2020. Phylogenetic and population genetic analyses reveal three distinct lineages of the invasive brown root-rot pathogen, *Phellinus noxius*, and bioclimatic modeling predicts differences in associated climate niches. Eur. J. Plant Pathol. 156:751-766.

Suárez, M. B., Diego, M., Feria, F. J., Martín-Robles, M. J., Moreno, S., and Palomo, J. L. 2022. New PCR-based assay for the identification of *Pectobacterium carotovorum* causing potato soft rot. Plant Dis. 106:676-684.

Thompson, J. D., Higgins, D. G., and Gibson, T. J. 1994. CLUSTAL W: Improving the sensitivity of progressive multiple sequence alignment through sequence weighting, position-specific gap penalties and weight matrix choice. Nucleic Acids Res. 22:4673-4680.

Tsai, J.-N., Ann, P.-J., Liou, R.-F., Hsieh, W.-H., and Ko, W.-H. 2017. *Phellinus noxius*: Molecular diversity among isolates from Taiwan and its phylogenetic

relationship with other species of *Phellinus* based on sequences of the ITS region. Bot. Stud. 58:9.

Tsai, J. N., Hsieh, W. H., Ann, P. J., and Yang, C. M. 2007. Development of specific primers for *Phellinus noxius*. Plant Pathol. Bull. 16:193-202.

Turechek, W. W., and Wang, H. 2023. Evaluation of a viable-cell detection assay for *Xanthomonas fragariae* with latent class analysis. PhytoFrontiers 3:214-224.

Tzean, Y., Shu, P.-Y., Liou, R.-F., and Tzean, S.-S. 2016. Development of oligonucleotide microarrays for simultaneous multi-species identification of *Phellinus* tree-pathogenic fungi. Microb. Biotechnol. 9:235-244.

Untergasser, A., Nijveen, H., Rao, X., Bisseling, T., Geurts, R., and Leunissen, J. A. M. 2007. Primer3Plus, an enhanced web interface to Primer3. Nucleic Acids Res. 35:W71-W74.

Wang, Y.-F., Meng, H., Gu, V. W., and Gu, J.-D. 2016. Molecular diagnosis of the brown root rot disease agent *Phellinus noxius* on trees and in soil by rDNA ITS analysis. Appl. Environ. Biotechnol. 1:81-91.

Whitchurch, C. B., Tolker-Nielsen, T., Ragas, P. C., and Mattick, J. S. 2002. Extracellular DNA required for bacterial biofilm formation. Science 295: 1487.

White, T. J., Bruns, T. D., Lee, S. B., and Taylor, J. W. 1990. Amplification and direct sequencing of fungal ribosomal RNA genes for phylogenetics. Pages 315-322 in: PCR Protocols: A Guide to Methods and Applications. M. A. Innis, D. H. Gelfand, J. J. Sninsky, and T. J. White, eds. Academic Press, San Diego, CA.

Wu, M. L., Chang, T. T., Jaung, L. M., Hung, T. H., Chen, C. H., and Lin, L. D. 2009. Establishment of PCR rapid detection technique for tree brown root rot disease. Quart. J. Chin. For. 42:239-247.

Wu, M. L., Chen, C. H., Chang, T. T., Jaung, L. M., and Hung, T. H. 2011. Establishment of the SOP of PCR detection techniques for brown root rot disease. Quart. J. Chin. For. 44:7-17.

Wu, Z.-C., Chang, Y.-Y., Lai, Q.-J., Lin, H.-A., Tzean, S.-S., Liou, R.-F., Tsai, I. J., and Chung, C.-L. 2020. Soil is not a reservoir for *Phellinus noxius*. Phytopathology 110:362-369.

Ye, J., Coulouris, G., Zaretskaya, I., Cutcutache, I., Rozen, S., and Madden, T. L. 2012. Primer-BLAST: A tool to design target-specific primers for polymerase chain reaction. BMC Bioinform. 13:134.

Zhou, L.-W., Ji, X.-H., Vlasák, J., and Dai, Y.-C. 2018. Taxonomy and phylogeny of *Pyrrhoderma*: A redefinition, the segregation of *Fulvoderma*, gen. nov., and identifying four new species. Mycologia 110:872-889.